On a circular cylinder in a steady wind at transition Reynolds numbers

By JOHN S. HUMPHREYS
AVCO Research and Advanced Development Division, Wilmington, Massachusetts

(Received 13 June 1960)

Some results of an experimental investigation of forces associated with the subsonic flow of air around a circular cylinder in a wind tunnel are presented. The oscillating forces due to the downstream vortex street are studied for Reynolds numbers in the 'critical' range 4×10^4 to 6×10^5. Of particular interest is the observation, at the onset of transition to turbulence, of a spanwise wave or cell pattern near the cylinder surface, which is stabilized in a striking manner by the use of fine threads as a visualization technique.

1. Introduction

The literature on the subject of eddy formation behind cylinders is quite extensive, dating back to Leonard da Vinci. Reviews have been given by Goldstein (1938), Rosenhead (1953), and Birkhoff & Zarantonello (1957), and an extensive one covering work up to 1958 was given by Humphreys (1959). The problem is still of interest because of the sometimes disturbing reaction of circular structures to natural flows, and because it has become possible through modern instrumentation to observe new details, such as the remarkable three-dimensional effects on average force and boundary-layer flow shown here.

A great deal of empirical information is available. The general eddy formation phenomenon (when compressibility effects are negligible) seems to fall into four regions in terms of Reynolds number $Re = \rho U_0 d/\mu$ (where U_0 is the free-stream velocity, d the cylinder diameter, ρ density and μ viscosity), which are not separated by clear boundaries but by transition zones that can, within limits, be altered by individual experimental conditions. These regions can be referred to by the terms symmetric, regular, irregular and supercritical, combining existing terminology. The symmetric range extends from Re about 5 to about 40, and is characterized by a lack of any oscillatory features. In the regular range, with Re between 50 and 140, the vortex motion is laminar and persists for a long distance downstream before being washed out by viscous diffusion.

The irregular region, extending over a wide range of Re from about 300 to 2×10^5 and containing many cases of engineering interest, is different in several respects. The wake contains considerable energy in the form of random turbulent fluctuations, and this can be explained in terms of a transition to turbulence of the free vortex layer that is still laminar as it leaves the cylinder. Due to mixing, the subsequent eddies of the turbulent fluid now die away much faster. Finally, above the 'critical' Re at about 3×10^5, where the C_D sharply drops, the wake is fundamentally turbulent and no definite vortices are observed. The turbulence originates in the cylinder boundary layer itself before it separates.

As yet the exact details of what occurs in the three transition zones are imperfectly understood. The highest zone, around the critical *Re*, is perhaps the most interesting in practice,* and new force and flow data are presented here for this region.

2. Force measurements

The apparatus used in the present study is shown schematically in figure 1, and was suspended in and above the test section of the closed circuit one-meter wind tunnel at Harvard University. A polished aluminium cylinder of 6 in.

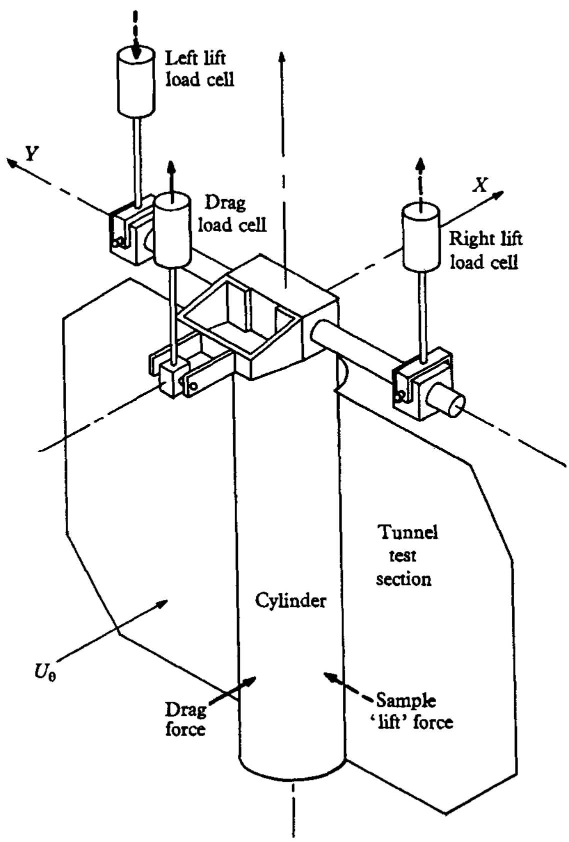

FIGURE 1. Diagram of force measuring system.

diameter was used for all of the results given here. It projected down through the tunnel roof and ended without support less than 0·05 in. off the floor of the test section. The tunnel itself can produce effective free-stream speeds in the test section from about 10 ft./sec to 200 ft./sec, which is still low enough to avoid serious compressibility effects. The force measurement system is built around

* Particularly to designers of large smokestacks, where vibration data at supercritical Reynolds numbers seem much more typical of the irregular region.

three strain-gauge 'load cells', which, when coupled to a high-gain carrier amplifier system, transmit to an oscillograph with very high sensitivity and linearity a record of the axial forces to which they are subjected.

If the wake oscillates regularly with frequency $f = \omega/2\pi$, and L is the cylinder length, then the side (or 'lift') force can be written as $C_K \times (\frac{1}{2}\rho U_0^2 Ld) \sin \omega t$, which defines the 'Karman coefficient' C_K (following Den Hartog 1954). The difference between the outputs of the two 'lift cells' then produces a measure of C_K, while the 'drag cell' output is directly related to the drag coefficient C_D. Calibration was done using static weights on the provisional (and normal) assumption that the phenomenon can be treated as a two-dimensional one, with uniform behaviour along the cylinder span. As described below, this is not in fact the case, so the resulting numbers are only averages over the span, and not simple linear averages at that, since the air forces are actually determined in

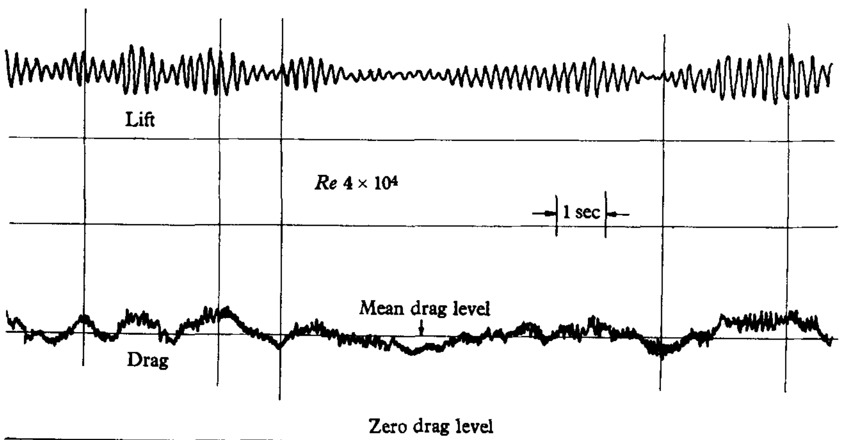

FIGURE 2. Oscillating lift and drag; sample record at subcritical Reynolds number.

terms of the moments that they produce at the support end of the cylinder. The tunnel turbulence level $(\overline{u^2})^{\frac{1}{2}}/U_0$ was found by hot-wire techniques to be close to 1 %, and was not noticeably affected by the presence of the cylinder.

On the hypothesis of a periodic two-dimensional wake, three force components are to be expected: a steady drag due to skin friction and wake underpressure, an oscillating lift at the eddy shedding frequency f due to gradients associated with vortex formation, and a small oscillating drag at frequency $2f$. All three of these quantities were measured by the author, with varying degrees of accuracy, for the range $3 \times 10^4 < Re < 6 \times 10^5$, thus spanning the upper critical Reynolds number region where wake periodicity breaks down. It can immediately be seen, however, from the tracing of a sample record shown in figure 2, that even at distinctly subcritical Re the situation is not as simple as might be hoped. There is superposed on both lift and drag a large-scale random fluctuation, which appears as a modulation of the lift oscillations and as a pronounced change (by as much as 15 %) in the net drag level. The lift modulation, which must be tied to a wake modulation, has been observed before by Roshko (1954), by

Macovsky (1958) and by Fung (1958), but no mention was made of the directly associated and quite significant drag changes. Any given single value, then, for C_D in the region just below critical Re can only be valid as an average over a suitably long period of time, here on the order of 20 sec.

Recognizing this, a mean C_D was determined for each record and is plotted in the usual way in figure 3, with several other curves due to previous workers (see Goldstein 1938 and Delany & Sorenson 1953) for comparison. The exact

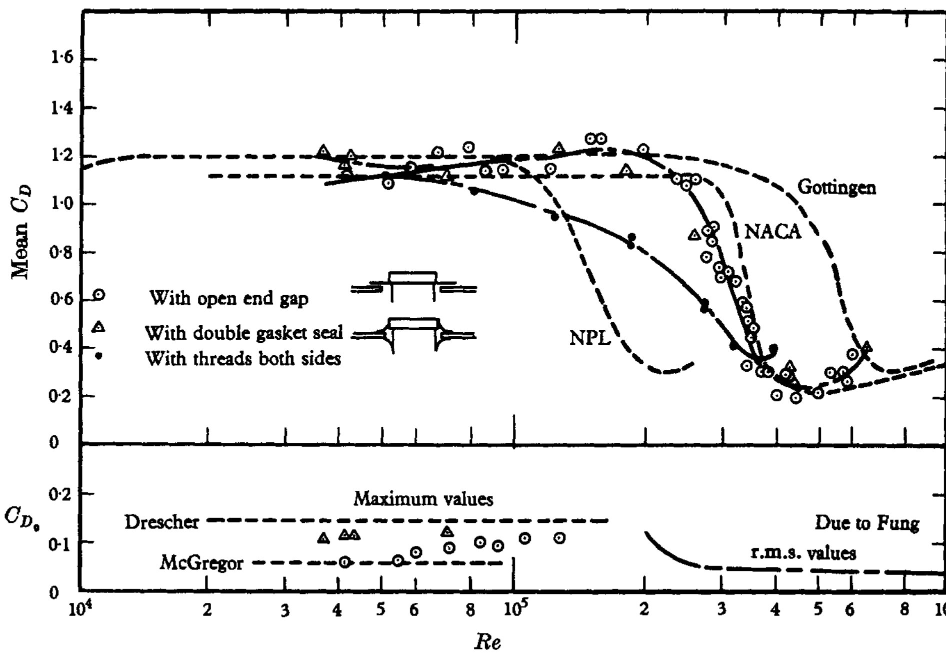

FIGURE 3. Mean and oscillating drag coefficient *vs* Reynolds number.

location of the sudden drop in C_D with increasing Re is understood to be a function of tunnel turbulence level, which determines at what speed the laminar to turbulent transition occurs in the cylinder boundary layer. The sudden narrowing of the wake following this transition provides an explanation for the connexion between drag changes and lift modulation at subcritical Re; both are simply a function of varying wake width. This is exaggerated in a closed tunnel test section (here the model occupies 16 % of the total cross-section area) by wake blockage effects.

A few points are presented in figure 3 for the maximum values of the double-frequency oscillating C_D (or C_{D_0}), but these amplitudes are close to the system noise level for subcritical Re, so accuracy is poor. Moreover, for Re in the critical range and above, this double frequency was close to a structural resonance, and the peak values are not plotted, since their validity would be dubious. Wave analyser studies, not presented here, have confirmed the observations of Fung (1958) that at supercritical Re no discernible peak is present in the frequency spectrum of C_D or C_K at the increased Strouhal numbers ($St = fd/U_0 = 0{\cdot}8$ and

0·4, respectively) that might be expected from reports of earlier hot-wire wake studies (see Goldstein 1938, p. 421, or Delany & Sorenson 1953).

Prior to 1958 there were made some estimates of the side (or 'lift') force, based either on amplitudes of cantilever cylinders vibrating near resonance, where self-excitation is crucial, or on space integrals or pressure distributions measured in various ways; much labour was involved in obtaining these estimates and the resulting points are few. These values of C_K vary from 0·6 (Drescher 1956) to 1·3 (McGregor 1957) for Re between 10^4 and 2×10^5.

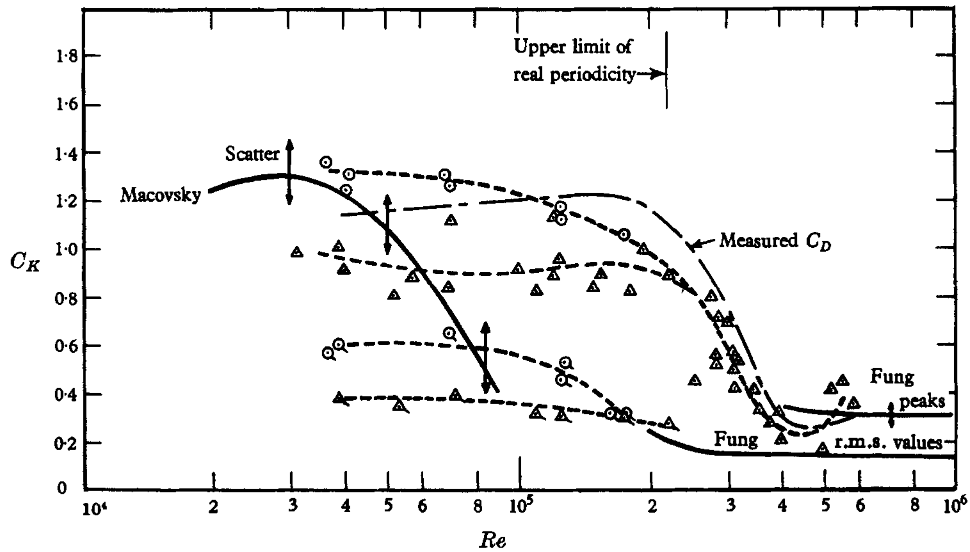

FIGURE 4. Karman lift coefficient *vs* Reynolds number. △ Maximum, △ mean, open end gap; ⊙ maximum, ⊙ mean, inside seal.

Some new data concerning the behaviour of the oscillating side force are shown in figure 4, in comparison with recent observations of Macovsky (1958) and Fung (1958), and some comments are required on the origin of these points. With the one exception of Fung (1958), all previously reported data on C_K have been in terms of 'maximum values', the information that is clearly of greatest interest to the smokestack designer, but which is somewhat ambiguous unless an explanation is given of just how this maximum was obtained. It is evident in most cases that this maximum is simply the largest fluctuation observed in the given run, but since random changes are involved here, the length of time of the run is definitely significant. If the result is based on only a few oscillations, as is the case with the earlier calculations based on pressures, then it is doubtful that the result is truly a representative maximum.

In the present case each of the points on figure 4 was computed from records containing (for subcritical Re) at least 500 complete oscillations, the maximum C_K being the largest seen on that record and the mean being the actual average of measured heights of on the order of 500 peaks. It must be mentioned that for Reynolds numbers in and above the critical region the measuring process used was very much more approximate, and even the definition of C_K becomes somewhat obscure, since there is no clearly periodic oscillation on which to base it. Still, it is not misleading to use the same symbol to refer to one-half of any single maximum peak-to-peak fluctuation, and this is what is given on figure 4. Since the author did not have available a really reliable meter capable of measuring (r.m.s.) averages over long times, no estimates of mean C_K at supercritical Re were made.

End conditions proved to be of unexpected importance. A number of different sealing arrangements were tried for the gap where the cylinder pierces the roof, with striking results of the sort shown in figure 4. Even the small geometry changes involved in replacing the plate by a flexible sponge-rubber collar type of seal (sketched in figure 3) were enough to shift the mean C_K by over 50 %. Since the force is measured in terms of the moment produced at the cylinder support, this effect is even stronger than it appears. Only one conclusion is possible. The change in end geometry must cause flow changes that are not confined to the end, but must affect the entire vortex shedding mechanism along the cylinder. This, in turn, must involve very considerable spanwise pressure gradients, and the whole basis for assuming two-dimensionality is thus thrown into question.

As the Reynolds number approaches the critical region it can be seen from figure 4 that the end effect becomes less and less apparent, which is reasonable since other disturbances become involved and an end disturbance will have relatively less importance. It is also clear from figure 3 that, while C_{D_0} is changed on a scale comparable to C_K, the mean C_D is affected hardly at all (about 5 % at $Re = 4 \times 10^4$). Neither observation lessens the implication that three-dimensional effects are of fundamental importance, and this prompted further investigation into the details of spanwise flow structure.

3. Observations on flow structure

The case of a straight cylinder mounted wall to wall across a symmetric wind tunnel (or water channel) has always been considered to be one of those in which a good argument can be made for eliminating the spanwise dimension. It is generally assumed that distributions in space and time of pressure and velocity measured at any station near the centre will suffice to characterize the entire flow.

There have been several suggestions in recent years that this assumption might not be entirely justified. Roshko (1954) notes a spanwise phase shift, implying periodic structure, in wake hot-wire signals at $Re = 80$, while Etkin, Korbacher & Keefe (1957) are able to explain a consistent discrepancy in acoustic radiation measurements between $Re\, 2 \times 10^4$ and 6×10^4 in terms of spanwise variations with a 'correlation length' of about $8d$. Macovsky (1958) observes large spanwise phase changes and flow components for $10^4 < Re < 10^5$, occurring at random and increasing in importance as Re approaches 10^5. Intuitively it is clear that this must indeed be the case as the transition to turbulent wake flow at critical Re is approached, since turbulence itself is fundamentally three-dimensional.

To visualize the flow character in the wake-forming region near critical Re, the most successful results in the present study were achieved by fastening a set of fine silk threads along the front stagnation line, which were long enough to extend around the surface just past the approximate location of turbulent

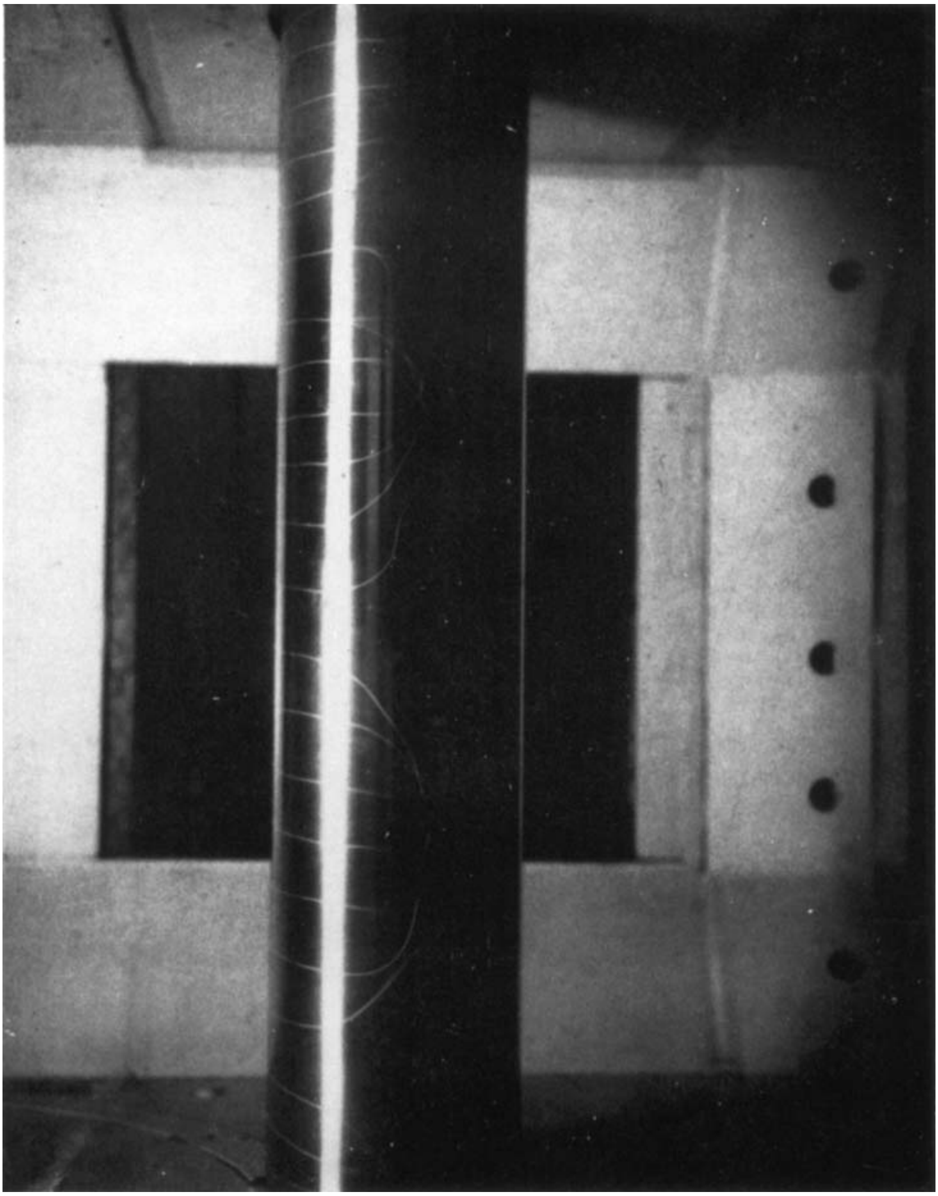

FIGURE 5 (plate 1). Surface thread patterns at critical Reynolds number showing spanwise cell structure.

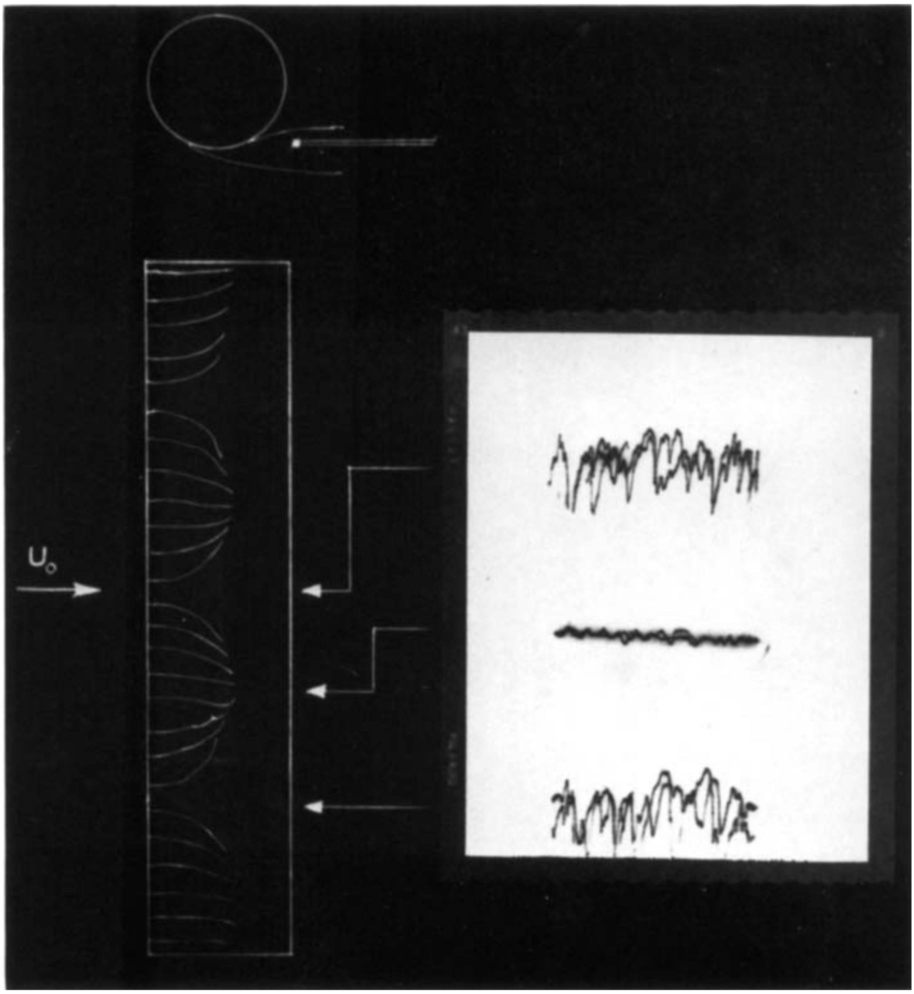

FIGURE 6 (plate 2). Hot-wire records of separated layer at critical Reynolds number, with threads showing spanwise cell structure.

(*a*) *Re* $2{\cdot}78 \times 10^5$ (*b*) *Re* $3{\cdot}06 \times 10^5$ (*c*) *Re* $3{\cdot}29 \times 10^5$ (*d*) with threads

FIGURE 7 (plate 2). Hot-wire correlations of separated layer from bare cylinder at critical Reynolds number; probes positioned as shown in figure 6.

boundary-layer separation (about 130°). For low speeds, the threads merely flap in and out with the wake, showing some spanwise irregularity but nothing that can be easily described or even photographed. When the speed is raised, however, to give a *Re* of about 10^5 (a point at which a vortex street is still definitely present for the bare cylinder) the remarkable phenomenon shown in figure 5 (plate 1) is observed.

A distinct wave or 'cell' pattern is formed by the threads; a pattern, moreover, which is very stable in time. It just moves slightly up and down, with the boundaries between cells sometimes becoming obscured or the individual cells briefly changing their size; but the central picture remains the same, even on changing end conditions or otherwise perturbing the wake flow. As the speed is increased the cells remain the same size, but the boundaries jump around with greater and greater rapidity, until by $Re\ 3 \times 10^5$ they are no longer visible. The pattern is not altered by the presence or absence of threads on the opposite side, or by locating a splitter plate in the wake, which essentially removes the vortex street. Thus the observed periodicity is not tied to wake periodicity.

In fact, at the velocity where the cell pattern first becomes clearly evident, the lift- and drag-force signals show that the oscillating lift has been practically eliminated and the C_D severely reduced, just due to the presence of the threads themselves. It is well known that increased surface roughness lowers the critical *Re* region in model tests (see Goldstein 1938, p. 432), and this is what seems to occur here, although as shown in figure 3 the effect of threads is really a broadening out of the critical region, rather than a displacement of it. Tests using different sizes of cylinders showed that the characteristic cell size is a function only of the cylinder diameter, and is between $1{\cdot}4d$ and $1{\cdot}7d$ in every case.

It is clear, then, that the cell pattern is associated with a 'critical' flow state, which means with the onset of transition from laminar to turbulent flow in the cylinder boundary layer. The cells then represent an intermediate state, which immediately suggests that perhaps the actual pattern is formed by the alternation of regions of laminar boundary-layer flow (early separation) with regions of turbulent boundary-layer flow (later separation). If this is so, then a hot wire traversed along the cylinder at a point that would be inside a laminar wake but outside a turbulent one should pass alternately through regions of agitated wake flow and smooth outer flow, and indeed it does. As expected, the cell maxima (or points towards which the threads bend) correspond to regions of delayed separation, hence turbulent flow, and it is not surprising to find that the end regions of the cylinder, with presumably greater disturbance levels present (due to wall boundary layers) are always cell maxima. Examples of the hot-wire signals received from a probe 1·2 in. from the surface at 139° from the stagnation point are shown in figure 6 (plate 2), the three positions corresponding to two cell minima and one maximum between.

This method immediately provides a way of answering the basic question whether the same type of cell formation exists at the lower edge of the critical *Re* region when the threads are removed. The author believes that a positive answer can be made to this question based on evidence that is qualitative in nature. There is no well-defined periodicity, and the cells of turbulence do not sit still, they move about on the surface; but they do appear to exist and to form the basic mechanism by which transition to turbulent boundary-layer flow is actually accomplished across the whole cylinder.

The same two hot wires were used in the same location as above with respect to the cylinder axis, and with a spanwise spacing approximately one half the cell size observed with threads attached. Simultaneous records were taken of the two signals, both on oscillograph paper and in the form of a 'correlation picture' obtained by letting each signal drive one set of plates on an oscilloscope. Four such pictures are shown in figure 7 (plate 2), along with the signal from each probe by itself as a function of time. Each picture is a triple exposure; at the top the signal from one probe for 0·2 sec, in the centre the other probe signal for a different 0·2 sec, and at the bottom a 15 sec correlation figure.

If the two signals were perfectly in phase, the correlation figure would be a straight line, while if they are both random and totally uncorrelated, the figure will be a circular spot with no clearly defined edge. Figure 7 (plate 2) shows three successive tunnel speeds (a, b and c) in the range where transition is partially established, together with a similar picture (d) for comparison, with threads on the cylinder and the cell pattern in evidence. The individual traces show periods of quiet flow and periods of large fluctuations succeeding each other fairly rapidly, thus suggesting the existence of moving turbulent cells. The lower figure tells in addition that this occurs quite closely out of phase, i.e. when one probe is experiencing laminar separation behaviour the other probe is (usually) experiencing the quiescent flow characteristic of turbulent separation. Of course, both signals could be small at once without changing the correlation pictures; but if they could also be both large at once, and in a random way, the figures would be much more uniformly filled in without such distinct points as are seen. The change from figure 7a to c is the sort of uniform transition toward greater dominance of turbulent separation (represented here by small signals) that is to be expected from the force data. On oscillograph records not shown here, it was possible to watch in a clearer way the progression from one hot wire to the other of these cells (or spots) of turbulence, whose motion and growth evidently make up the phenomenon of transition.

With this picture of what is taking place in the cylinder boundary-layer flow, a simple plausible explanation can be given of why cells of a particular size are maintained by the presence of fine threads. For regions where the flow in the boundary layer has become turbulent, the separation point is delayed compared to laminar regions, and there is associated with this a marked change in the surface normal pressure distribution, as is well known (e.g. see Goldstein 1938, p. 422). For stations at angles between 30° and 120° from the front stagnation point, the normal pressure is greater if the boundary layer remains laminar before separation than it is if it becomes turbulent, and it was experimentally confirmed that this is true while the thread cell pattern is present. Along any one generator in this section of the surface at a given time, there exist pressure differences and hence accelerations in the flow, directed from the laminar to the turbulent regions, thus moving the fine threads in the directions seen. But the threads do not have negligible inertia, moreover, they tend to catch on small surface irregularities, the net effect being a 'tripping' of the cross-flow which can trigger the transition to turbulence and preserve the status of the turbulent regions.

The choice of a preferred cell size can be crudely justified by noting that the simplest curve joining the boundaries of a cell without discontinuities or flat spots is a semicircle, and in fact at many times the actual boundary comes close to this shape (see figure 5, plate 1). To fit a semicircle onto the surface between 30° and 120°, where pressure differences exist, requires a spanwise distance of $\frac{1}{2}\pi d$, or $1{\cdot}56d$, which agrees very well with observation.

4. Corrections to velocity and force values

In the determination here of an effective free-stream velocity, corrections have been made for compressibility, contraction losses, solid blockage and wake blockage. Calculations of average force coefficients include a transmissibility correction for the cylinder flexibility, and are based on an effective cylinder length that makes allowance for the wall boundary layers. Known errors in the velocity determination add up to about $\pm 8\,\%$. The data (past and present) as shown graphically does not always indicate these tolerances.

As a result of the large spanwise changes seen here, there might be considerable doubt whether the lift-force modulations seen at lower Reynolds number are really modulations of average force in space instead of time, since net forces are actually read out in terms of support moments. To check this, the structure was modified to measure C_K directly, with results that were not appreciably different from earlier records, implying that the fluctuations in C_K indeed are due to time variation of the whole vortex street flow.

5. Conclusions

From the data summarized above it is clear that flow changes in the spanwise direction, which are commonly neglected, are of crucial importance in determining the nature of fluid flow in the wake-forming region behind a circular cylinder. For Reynolds numbers just below 10^5, where a definite vortex street exists, the maximum side force at the eddy frequency is comparable to the mean drag, C_K rising as high as $1{\cdot}3$ (confirming other results); but this is highly dependent on specific details of the end conditions. The breakdown of the periodic wake into a turbulent one, with large concurrent drops in both force coefficients, has long been connected with boundary-layer transition prior to separation; but here this has been explored further and specifically tied to the appearance of a particular kind of mixed flow. With threads on the cylinder surface, this becomes a stable spanwise pattern of cells in the boundary layer, and further hot-wire results have led to the conclusion that such cells, composed of turbulent fluid and of various and varying sizes, are for the bare cylinder the first sign of developing transition at critical Reynolds number.

This work forms part of a thesis submitted to Harvard University in partial fulfilment of the requirements for the Ph.D. degree; see Humphreys (1959). The helpful advice of Prof. R. E. Kronauer throughout the work is gratefully acknowledged.

REFERENCES

Birkhoff, G. & Zarantonello, E. 1957 *Jets Wakes and Cavities*, chapter 13. New York: Academic Press Inc.

Delany, N. & Sorenson, N. 1953 *NACA TN* 3038.

Den Hartog, J. P. 1954 *Proc. Nat. Acad. Sci., Wash.*, **40**, 3, 155.

Drescher, H. 1956 *Z. Flugwis*, **4**, 17.

Etkin, B., Korbacher, G. & Keefe, R. 1957 *J. Acoust. Soc. Amer.* **29**, 30.

Fung, Y. C. 1958 *Space Tech. Labs. Rep.* GM-TR-0165-00343, also 1960, *J. Aero. Sci.*, to be published.

Goldstein, S. 1938 *Modern Developments in Fluid Mechanics.* Oxford University Press.

Humphreys, J. 1959 *On a Circular Cylinder in a Steady Wind.* Harvard University Ph.D. Thesis in Mechanical Engineering.

Macovsky, M. 1958 *Vortex Induced Vibration Studies.* U.S. Navy Dept., D. Taylor Model Basin, Rep. 1190.

McGregor, D. 1957 *Experimental Investigation of Oscillating Pressures on a Circular Cylinder in a Fluid Stream.* University Toronto Inst. Aerophys., TN, no. 14.

Rosenhead, L. 1953 *Vortex Systems in Wakes*, p. 185. Adv. in Appl. Mech. III, Academic Press.

Roshko, A. 1954 On the Development of Turbulent Wakes from Vortex Streets. *NACA Rep.* 1191.